Robust Responses of the Hydrological Cycle to Global Warming

Isaac M. Held

National Oceanic and Atmospheric Administration/Geophysical Fluid Dynamics Laboratory, Princeton, New Jersey

Brian J. Soden

Rosenstiel School for Marine and Atmospheric Science, University of Miami, Miami, Florida

ABSTRACT

Using the climate change experiments generated for the Fourth Assessment of the Intergovernmental Panel on Climate Change, this study examines some aspects of the changes in the hydrological cycle that are robust across the models. These responses include the decrease in convective mass fluxes, the increase in horizontal moisture transport, the associated enhancement of the pattern of evaporation minus precipitation and its temporal variance, and the decrease in the horizontal sensible heat transport in the extratropics. A surprising finding is that a robust decrease in extratropical sensible heat transport is found only in the equilibrium climate response, as estimated in slab ocean responses to the doubling of CO_2, and not in transient climate change scenarios. All of these robust responses are consequences of the increase in lower-tropospheric water vapor.

1. Introduction

There remains considerable uncertainty concerning the magnitude of the temperature response to a given increase in greenhouse gases. But there are a number of climatic responses that are tightly coupled to the temperature response. Most of these are related, directly or indirectly, to lower-tropospheric water vapor. We are confident that lower-tropospheric water vapor will increase as the climate warms. We can predict, with nearly as much confidence, that certain other changes will occur that are coupled to this increase in water vapor. In this article we describe some of these robust hydrological responses to warming.

We use the archive of coupled climate models results organized by the Program for Climate Model Diagnosis and Intercomparison (PCMDI) for the Fourth Assessment Report (AR4) of the Intergovernmental Panel on Climate Change as our primary tool in assessing robustness. Some aspects of the hydrological responses to warming are consistent among these models and some

are not. To study the latter requires one to understand the consequences of different model formulations, often at a detailed level. When studying a consistent part of the response, in contrast, one is not concerned with the specifics of individual models, but with providing simple physical arguments that add additional support for the plausibility of the response. Some of these robust responses to warming are already well appreciated, but we gather several together here, partly for pedagogical reasons, and partly with the hope of motivating new observational studies to determine whether these responses, which the models predict are already occurring, are detectable.

As in many discussions of water vapor and global warming, our starting point is the Clausius–Clapeyron (CC) expression for the saturation vapor pressure:

$$\frac{d \ln e_s}{dT} = \frac{L}{RT^2} \equiv \alpha(T), \tag{1}$$

where L is the latent heat of vaporization and R is the gas constant. At temperatures typical of the lower troposphere, $\alpha \approx 0.07 \text{ K}^{-1}$; the saturation vapor pressure increases by about 7% for each 1-K increase in temperature. If the equilibrium response of lower-tropospheric temperatures to a doubling of CO_2 is close to the canonical mean value of 3 K, this corresponds to

Corresponding author address: Dr. Brian J. Soden, Rosenstiel School for Marine and Atmospheric Science, University of Miami, 4600 Rickenbacker Causeway, Miami, FL 33149.
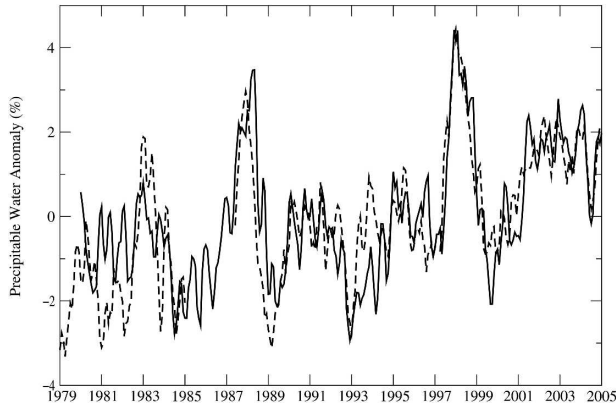E-mail: b.soden@miami.edu

FIG. 1. A time series of the tropical-mean (30°N–30°S), ocean-only column-integrated water vapor from satellite observations (dashed) and GFDL GCM simulations with prescribed SST (solid). The satellite observations for 1979–84 are from the SMMR (Wentz and Francis 1992) and for 1987–2004 are from the SMM/I (Wentz 1997). The mean seasonal cycle is removed from both the observations and model simulations, and the SMMR anomalies are adjusted such that their mean equals that of the model for their overlapping time period (1980–84). All time series are smoothed using a 3-month running mean.

a 20% increase in e_s. Given the size of this increase, it is important to understand which aspects of the climate response are tightly coupled to the increase in e_s and which are not. We discuss the increase in column-integrated water vapor, the decrease in convective mass fluxes, the increase in horizontal moisture transport, the associated enhancement of the pattern of evaporation minus precipitation and its temporal variance, and the decrease in horizontal sensible heat fluxes in the extratropics (in steady state), all of which are robust responses to the increase in temperature and e_s.

2. Column-integrated water vapor

Before turning to the coupled model results, we show in Fig. 1 a time series of the ocean-only tropical-mean column-integrated water vapor based on microwave satellite measurements from the Scanning Multichannel Microwave Radiometer (SMMR; Wentz and Francis 1992) and the Special Sensor Microwave Imager (SSM/I; Wentz 1997). Also shown is the corresponding simulated time series, using a version of the AM2/LM2 developed at the Geophysical Fluid Dynamics Laboratory (GFDL Global Atmospheric Model Development Team 2004). No external parameters or forcing agents are changing in time, except for the lower boundary condition, which is the observed sea surface temperatures (and sea ice). The quality of the agreement is consistent with a very tight relation between sea surface

temperatures and integrated water vapor (Wentz and Schabel 2000; Trenberth et al. 2005). Interannual variability, dominated by ENSO events and the longer-term trend, is captured with some fidelity.

It is well known that climate models tend to maintain a fixed tropospheric relative humidity as they warm. The modest changes in relative humidity that the models do generate are worthy of study, but they are too small to substantially modify the increase in column-integrated vapor resulting from the increase in saturation vapor pressure. The data in Fig. 1 do not raise any concerns in this regard, over the tropical oceans at least.

It is perhaps worth emphasizing that column-integrated vapor is dominated by the lower troposphere, whereas infrared water vapor feedback is dominated by the upper tropical troposphere (see Held and Soden 2000). Our focus here is not on water vapor feedback nor on climate sensitivity but on the hydrological response given a lower-tropospheric temperature change.

Using the PCMDI/AR4 archive we examine the change in climate in the A1B scenario between the first 20 yr and the last 20 yr of the twenty-first century. We consider only one realization from each of 20 models (listed in Table 1). Figure 2a shows the globally averaged total column water vapor plotted against the global-mean surface air temperature increase. Not surprisingly, climate models obey CC scaling fairly closely. A linear fit has a slope that is slightly greater than what one would expect from CC scaling with global-mean surface air temperature.

Figure 2c shows the results obtained from the 20C3M simulations of the years 1860–2000, using the difference between the first 20 yr and the last 20 yr of the twentieth century. The result is nearly identical to that obtained from the twenty-first-century projections, with CC scaling fitting the results quite well. The larger spread in the temperature responses in this figure is in part a consequence of a larger contribution from noise as compared to the smaller forced response. The fact that the correlation is nearly as tight as in the twenty-first-century integrations suggests that temperature fluctuations generated internally are also accompanied by CC scaled water vapor fluctuations, consistent with the GFDL AM2/LM2 results in Fig. 1 on shorter time scales.

3. The global-mean hydrological cycle

It is important that the global-mean precipitation or evaporation, commonly referred to as the strength of the hydrological cycle, does *not* scale with Clausius–Clapeyron (see also Betts 1998; Boer 1993; Trenberth

TABLE 1. A list of PCMDI AR4 model simulations used in the analysis of the 20C3M and SRES A1B scenarios. Some models are omitted from figures due to missing variables.

Model	Modeling center
BCCR BCM2	Bjerknes Center for Climate Research
CCCMA CGCM3	Canadian Centre for Climate Modelling and Analysis
CNRM CM3	Center National de Recherches Meteorologiques
CSIRO Mk3	Commonwealth Scientific and Industrial Research Organisation (CSIRO) Atmospheric Research
GFDL CM2.0	Geophysical Fluid Dynamics Laboratory
GFDL CM2.1	Geophysical Fluid Dynamics Laboratory
GISS AOM	Goddard Institute for Space Studies
GISS EH	Goddard Institute for Space Studies
GISS ER	Goddard Institute for Space Studies
IAP FGOALS1	Institute for Atmospheric Physics
INM CM3	Institute for Numerical Mathematics
IPSL CM4	Institut Pierre Simon Laplace
MIROC(hires)	Center for Climate System Research
MIROC(medres)	Center for Climate System Research
MIUB ECHO	Meteorological Institute University of Bonn
MPI ECHAM5	Max Planck Institute for Meteorology
MRI CGCM2	Meteorological Research Institute
NCAR CCSM3	National Center for Atmospheric Research
NCAR PCM1	National Center for Atmospheric Research
UKMO HadCM3	Met Office's Hadley Centre for Climate Prediction

1998; Allen and Ingram 2002). Figures 2b–d show how this strength of the global hydrological cycle responds to warming in the A1B scenario and in the 20C3M simulations in the AR4 archive. While there is an increase in strength that is correlated with increased temperature across the models, there is substantial scatter and, more importantly, the sensitivity is on the order of 2% K^{-1} (with a median value of 1.7% K^{-1}), much weaker than CC scaling. In the twentieth century, precipitation is reduced rather uniformly below the fit for the twenty-first-century projections by about 1%. As a result, it is only the models that warm the most strongly that clearly show an increase in precipitation over the twentieth century. We presume that this ~1% reduction is due to an increase over the century in absorbing aerosols (Ramanathan et al. 2001).

The change in global-mean precipitation, or evaporation, can be decomposed into a part associated with the change in Bowen's ratio and a part due to the net change in radiative flux at the surface. Using an atmospheric model (GFDL Global Atmospheric Model Development Team 2004), we have computed instantaneous radiative flux perturbations created by increasing atmospheric and surface temperatures throughout the troposphere by 1 K, holding relative humidity and clouds fixed. Averaging over a year and the globe, the result is an increase of only 0.7 W m^{-2} in the net downward radiation at the surface. The increase in absorbed solar flux associated with the reduction in surface albedo is ~0.3 W m^{-2} K^{-1} warming averaged over the

AR4 models (Soden and Held 2006; Winton 2006). The combination of the radiative effect of uniform warming and the increase in albedo can explain at best 1 W m^{-2}, or about a 1% K^{-1} increase. A doubling of CO_2 holding the atmospheric state fixed increases the net flux by 0.66 W m^{-2}, or roughly 0.7%, but this term should cause a small positive intercept along the precipitation axis in Fig. 2b rather than a change in slope. A decrease in Bowen's ratio plays a significant role in generating the δP versus δT slope generated by the models, but it also cannot compete with CC scaling; the latent heating is already dominant over the sensible, so there is little room for an increase with fixed radiative flux. Cloud feedbacks likely contribute to the scatter among the models. In any case, a sensitivity smaller than that implied by CC scaling is clearly to be expected. [For reasons that are unclear, some one-dimensional radiative–convective models predict sensitivities of the global hydrological cycle as large as 4% K^{-1} (Lindzen et al. 1982; Pierrehumbert 2002).]

4. Mass exchange between the boundary layer and free troposphere

The fact that the strength of the global-mean hydrological cycle increases more slowly than does the mixing ratio near the surface has important consequences for the atmospheric circulation (Betts 1998). We can think of parcels of air leaving the boundary layer for the free
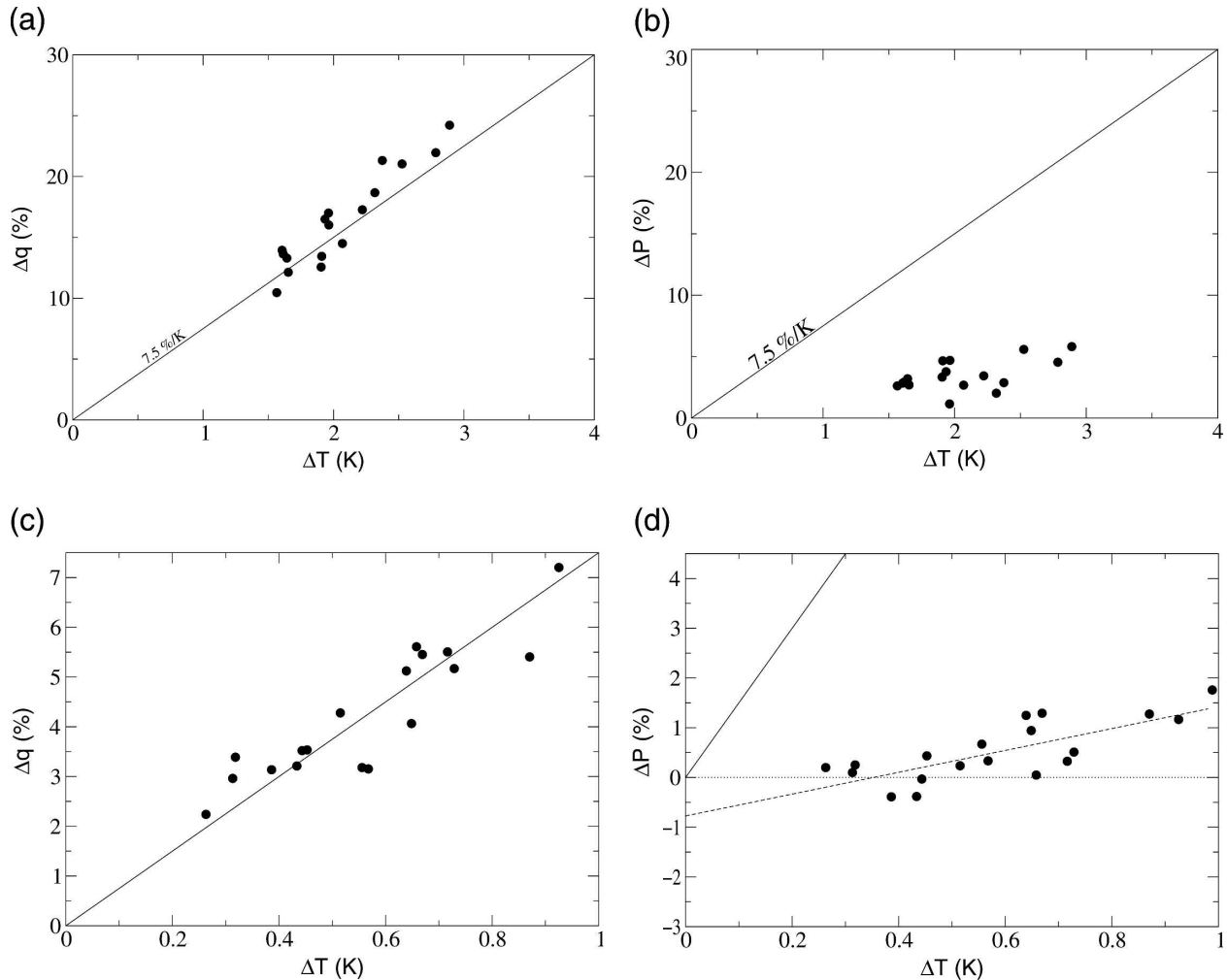
FIG. 2. Scatterplot of the percentage change in global-mean column-integrated (a),(c) water vapor and (b),(d) precipitation vs the global-mean change in surface air temperature for the PCMDI AR4 models under the (a),(b) Special Report on Emissions Scenarios (SRES) A1B forcing scenario and (c),(d) 20C3M forcing scenario. The changes are computed as differences between the first 20 yr and last 20 yr of the twenty-first (SRES A1B) and twentieth (20C3M) centuries. Solid lines depict the rate of increase in column-integrated water vapor (7.5% K^{-1}). The dashed line in (d) depicts the linear fit of ΔP to ΔT, which increases at a rate of 2.2% K^{-1}.

troposphere carrying large boundary layer mixing ratios, condensing and precipitating much of this vapor, and returning with much smaller vapor content. If we ignore this return flow of vapor, we have simply, in the global mean, $P = Mq$, where P is the precipitation, M is the mass exchanged per unit time, and q is a typical boundary layer mixing ratio. (The mass flux in nonprecipitating shallow convection should be excluded from M.) Since q scales with CC but P increases more slowly, M must decrease rapidly, albeit a bit less rapidly than the CC rate. There are a number of ways of measuring the strength of the atmospheric circulation, but by this particular measure, the circulation must weaken as the climate warms. We can, alternatively, speak of the

mean residence time of water vapor in the troposphere as increasing with increasing temperature (Roads et al. 1998; Bosilovich et al. 2005).

Since the bulk of the evaporation and precipitation occurs in the Tropics, this argument is relevant for the Tropics in isolation. We therefore expect the mass flux in precipitating convective towers to decrease with increasing temperature. In most comprehensive climate models, this convective mass flux is not explicitly simulated by the resolved motions but is estimated by subgrid-scale closure theories. One might think that little confidence should be placed in the rate of change of convective mass transport with increasing temperature predicted by these models, given the uncertainties in
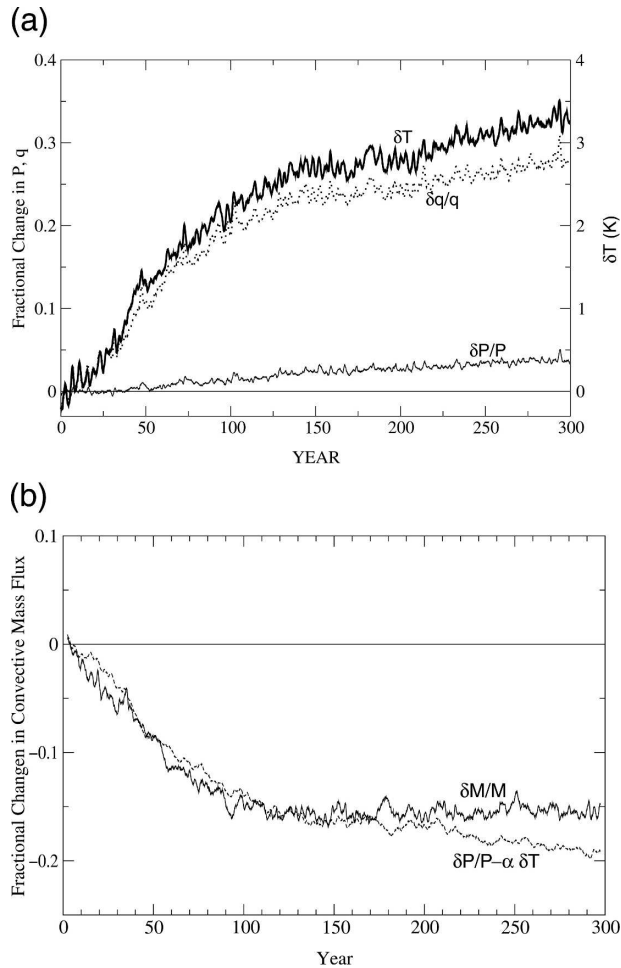
(a)

(b)

FIG. 3. (a) The change in global-mean surface air temperature, δT (solid), fractional change in precipitation, $\delta P/P$ (dashed), and column-integrated water vapor, $\delta q/q$ (dotted). (b) The fractional change in global-mean convective mass flux $\delta M/M$ (solid) and the corresponding change in $\delta P/P - \alpha \delta T$ (dashed). All results are from the GFDL CM2.1, and the time series are smoothed using a 5-yr running mean.

these closure theories. But the constraints described above operate in the models whether or not the mass flux is resolved by the model or contained in the subgrid-scale closure. Figure 3a is a plot of the time evolution of the fractional changes in global-mean precipitation and column-integrated water vapor. Figure 3b is the corresponding plot of the global-mean subgrid-scale convective mass flux in GFDL's CM2.1 model at 500 mb as a function of time in its A1B scenario, and that predicted from P/q assuming that q follows CC scaling at 7% K^{-1} and taking P from the model: $\delta M/M = \delta P/P - 0.07\delta T$. The temperature change δT and the fractional precipitation change $\delta P/P$ are also shown in the figure.

We do not have access to the convective mass fluxes

from most of the models in the PCMDI/AR4 archive to test directly for the robustness of this result, but to the extent that one can simply set $M \propto P/q$, the results in Fig. 2 show that this mass flux decreases in all models.

The reduced upward convective mass flux implies a reduction in the compensating radiatively induced subsidence in the Tropics. An alternative argument for weaker tropical mass exchange is provided by Knutson and Manabe (1995), who focus on the compensating subsidence. Temperatures in the Tropics are dynamically constrained to be very uniform above the planetary boundary layer. In the deep convecting regions, the atmosphere is close to the moist adiabat determined by the moisture content in the boundary layer in those regions. In nonconvecting regions, the free-tropospheric temperatures must be close to the same moist adiabat. [See Santer et al. (2005) for confirmation that the AR4 models behave in this simple way.] In regions with no deep convection, the radiative cooling Q balances the adiabatic warming associated with the subsidence: $Q = \omega \partial\theta/\partial p$, where θ is the potential temperature and ω is the vertical p velocity. On a moist adiabat, $\partial\theta/\partial p$ averaged over the troposphere is proportional to Lq, where q is the boundary layer mixing ratio. The dry stability in the model Tropics increases as the temperature and the low-level moisture increase, following CC scaling. Since $Q \approx P$ the radiative cooling of the troposphere does not increase as rapidly as the increase in stability, and the subsidence weakens, at the rate of $\delta\omega/\omega \approx \delta P/P - \delta q/q$, just as before.

The observed trend over the past two decades in the tropical lapse rate remains a subject of controversy (see Santer et al. 2005). In the context of this paper, we provisionally assume that this controversy will be settled in favor of a tropical atmosphere that stays close to a moist adiabat. Otherwise the models are seriously deficient, and aspects of these arguments will need to be revisited.

A reduction in the mass exchange in the Tropics does not necessarily entail a proportional reduction in the strength of the mean tropical circulation. In the idealized problem of horizontally homogeneous radiative convective equilibrium, there is no mean circulation, yet the argument presented continues to hold and one still expects a reduction in convective mass flux with increasing temperature. One can think of the mean circulation as the superposition of a radiatively driven subsidence and an upward convective mass flux. Redistribution of the latter can change the strength of the circulation independently of the radiatively driven subsidence.

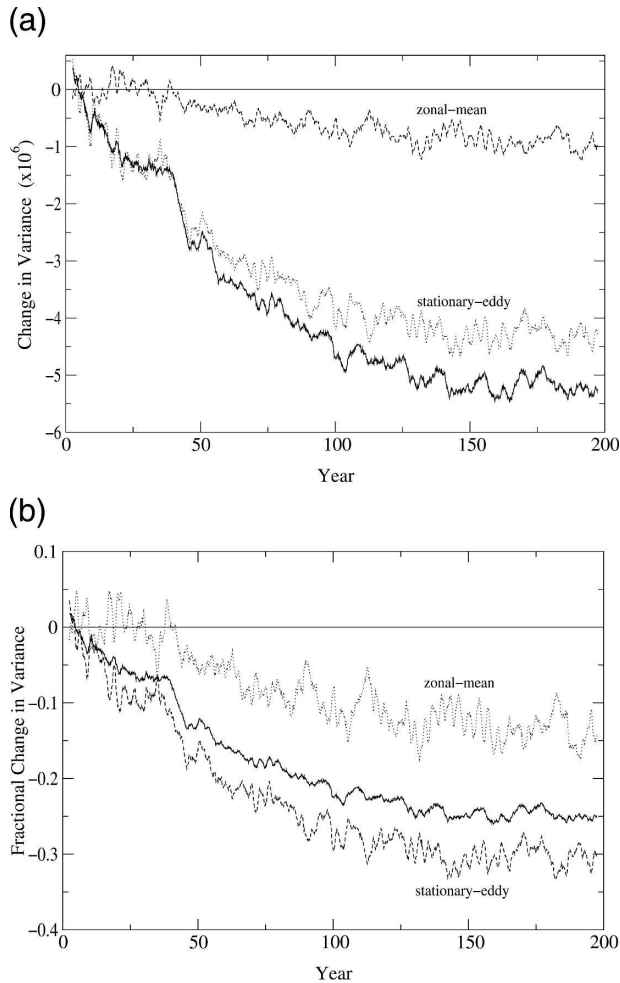The spatial variance over the Tropics of the convec-

(a)

(b)

FIG. 4. Time series of the (a) absolute and (b) fractional change in spatial variance of monthly mean convective mass flux at 500 mb over the Tropics. Results are shown separately for the total (solid), zonal-mean (dashed), and eddy (dotted) components of the variance. All results are from the GFDL CM2.1, and the time series are smoothed using a 5-yr running mean.

tive mass flux is a convenient measure of the strength of the circulation driven by convection. If the reduction in the mass flux is everywhere proportional to the preexisting mass flux, then the variance should decrease at twice the rate of the mean mass flux: $2(\delta P/P - \delta q/q) \cong$ 10% K^{-1}. The rate of reduction in CM2.1 (Fig. 4) is ~25% for a ~3-K warming, somewhat smaller than the expectation based on a proportional reduction, indicating that there is modest redistribution of convection toward less uniformity, causing the circulation to weaken more slowly than one would expect based on the total mass flux scaling itself. (In this calculation, we compute the variance for each monthly mean and then average over time, and define the Tropics to be be-

tween 30°N and 30°S). We can divide this variance of the tropical convective mass flux into a part due to the zonal-mean mass flux and a part due to the stationary eddy mass flux (we refer to this eddy contribution as due to "stationary" eddies since we start with monthly mean data). One can then ask if the reduction in variance takes place in the stationary eddy component or in the zonal mean. (In CM2.1, the zonal-mean variance accounts for 40% of the total variance.) As the climate warms, the reduction in total variance is dominated by a reduction of the stationary eddy component (Fig. 4a). The fractional reduction (Fig. 4b) in the stationary eddy component (10% K^{-1}) is consistent with CC scaling, while the fractional reduction in the zonal-mean component (4% K^{-1}) is substantially smaller than that expected from CC scaling.

The implication is that the *redistribution* of convection is such as to increase the variance of the zonal mean, so that the circulation consistent with this component, the zonal-mean Hadley cell, does not decrease in strength as fast as CC scaling of the mass flux would suggest. See Mitas and Clement (2005) for a discussion of the modest weakening of the (wintertime) Hadley cell in most of the AR4 models. We suspect that the zonal-mean Hadley cell is restricted by other factors from decreasing in strength as strongly as implied by the CC scaling of the mass flux

Mitas and Clement (2005) also discuss the trend toward *increasing* strength of the Hadley cell in the National Centers for Environmental Prediction–National Center for Atmospheric Research (NCEP–NCAR) reanalysis and 40-yr European Centre for Medium-Range Weather Forecasts (ECMWF) Re-Analysis (ERA-40) over the past 20 yr. We are aware of no models that simulate such an increase, but it would not necessarily be inconsistent with our line of argument if there were sufficient reorganization of the convection strengthening meridional contrasts at the expense of zonal contrasts. But our tentative working hypothesis is that these trends are artifacts of the reanalysis related to the fact that the tropical lapse rate in the radiosonde data is increasing (Santer et al. 2005) rather than staying close to a moist adiabat. Inappropriately nudging a model toward a more unstable tropical lapse rate in an analysis cycle, by this hypothesis, will result in an artificial increase in convection and artificial intensification of the Hadley cell.

5. Moisture transport

A very important consequence of the increase in lower-tropospheric water is the increase in horizontal

vapor transport within the atmosphere. Consider the time-averaged, vertically integrated, horizontal transport of vapor F. The convergence of this transport balances the difference between evaporation and precipitation. A seemingly simplistic but useful starting point for discussion is the assumption that the response of F is everywhere dominated by the change in lower-tropospheric mixing ratios rather than changes in the flow field, so that the transport also exhibits CC scaling:

$$\frac{\delta F}{F} \approx \frac{\delta e_s}{e_s} \approx \alpha \delta T. \tag{2}$$

The relevant temperature change is the change in the lowest 2 km or so since this is where the bulk of the water vapor resides.

A somewhat different argument can be made based on a simple diffusive picture of midlatitude eddy fluxes. If moisture and temperature are diffused with the same diffusivity, then the ratio of the latent heat transport $F_L = LF$ to the sensible heat transport F_S will be the ratio of the gradient of $c_p T$ to the gradient of $Lq = Lhq_s$, where h is the relative humidity (assumed to be constant once again). Setting $(\partial q_s/\partial y) = (dq_s/dT)(\partial T/\partial y)$ and $\xi \equiv (L/c_p)(dq_s/dT)$, we have $F_L/F_S = h\xi$. As temperatures increase, ξ increases, and the fractional change in the moisture transport is

$$\frac{\delta F_L}{F_L} = \frac{\delta F_s}{F_s} + \frac{\delta \xi}{\xi} \approx \frac{\delta F_s}{F_s} + \frac{1}{\xi}\frac{d\xi}{dT}\delta T = \frac{\delta F_s}{F_s} + \frac{d^2 e_s/dT^2}{de_s/dT}\delta T. \tag{3}$$

Since the temperature dependence of e_s is predominately exponential, the ratio of the second derivative of e_s to its first derivative is essentially α once again:

$$\frac{\delta F_L}{F_L} \approx \frac{\delta F_S}{F_S} + \alpha \delta T. \tag{4}$$

If one assumes that the eddy sensible heat transport does not change, one finds a similar result to that obtained above with the simpler assumption of fixed flow. We return to the relationship between latent and sensible transports below.

We compute δF per unit global warming in each of the AR4 integrations and then average over the model ensemble and plot the result in Fig. 5a. Also shown is the simple prediction, $\alpha \delta T F$, where δT is the zonal- and annual-mean temperature change per unit global warming. (We compute this estimate for each model and then average over all models.) For Fig. 5b, we locate the midlatitude maximum in the annual-mean
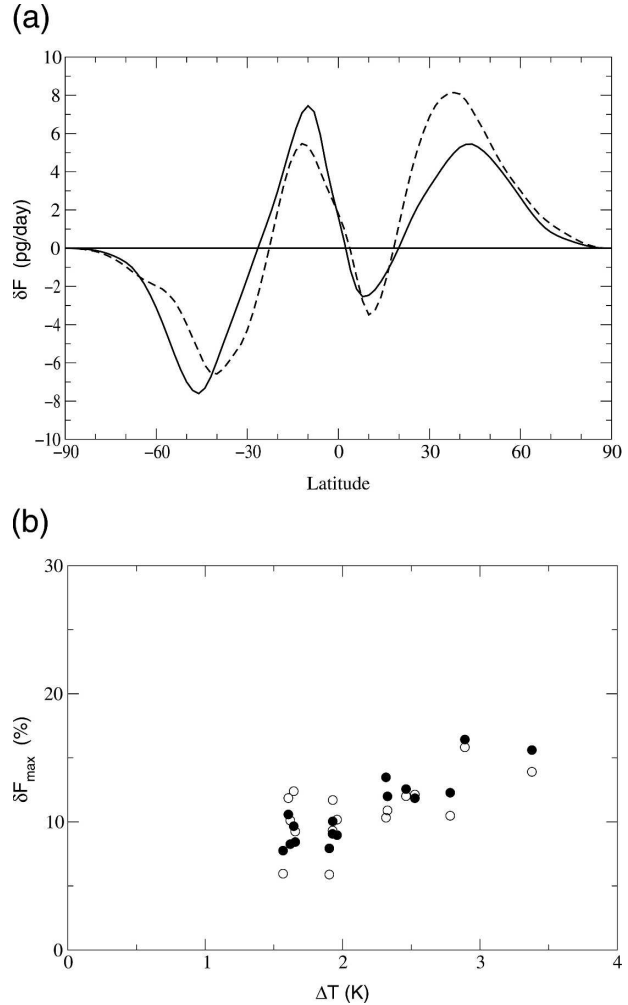

FIG. 5. (a) The change in zonal-mean northward moisture transport, F, from the ensemble mean of PCMDI AR4 models under SRES A1B scenario (solid) and the corresponding thermodynamic contribution (dashed) predicted from (2). (b) Scatterplot of the percentage change in the maximum poleward moisture transport, F_{max}, vs the global-mean δT for individual models. Results are shown separately for the Northern Hemisphere (filled) and Southern Hemisphere (open).

poleward moisture transport in each model (and each hemisphere) and plot the fractional change in this flux at this latitude in the A1B scenario, as a function of the change in global-mean surface temperature. Despite some scatter, the correlation is clear, with a slope of roughly 5% K^{-1}. If one plots against the temperature change at this latitude, rather than the change in global-mean temperature, the slope in the Northern Hemisphere is reduced (to roughly 4% K^{-1}) while the slope in the Southern Hemisphere is increased. The quantitative departures from precise CC scaling are significant, especially in the Northern Hemisphere when
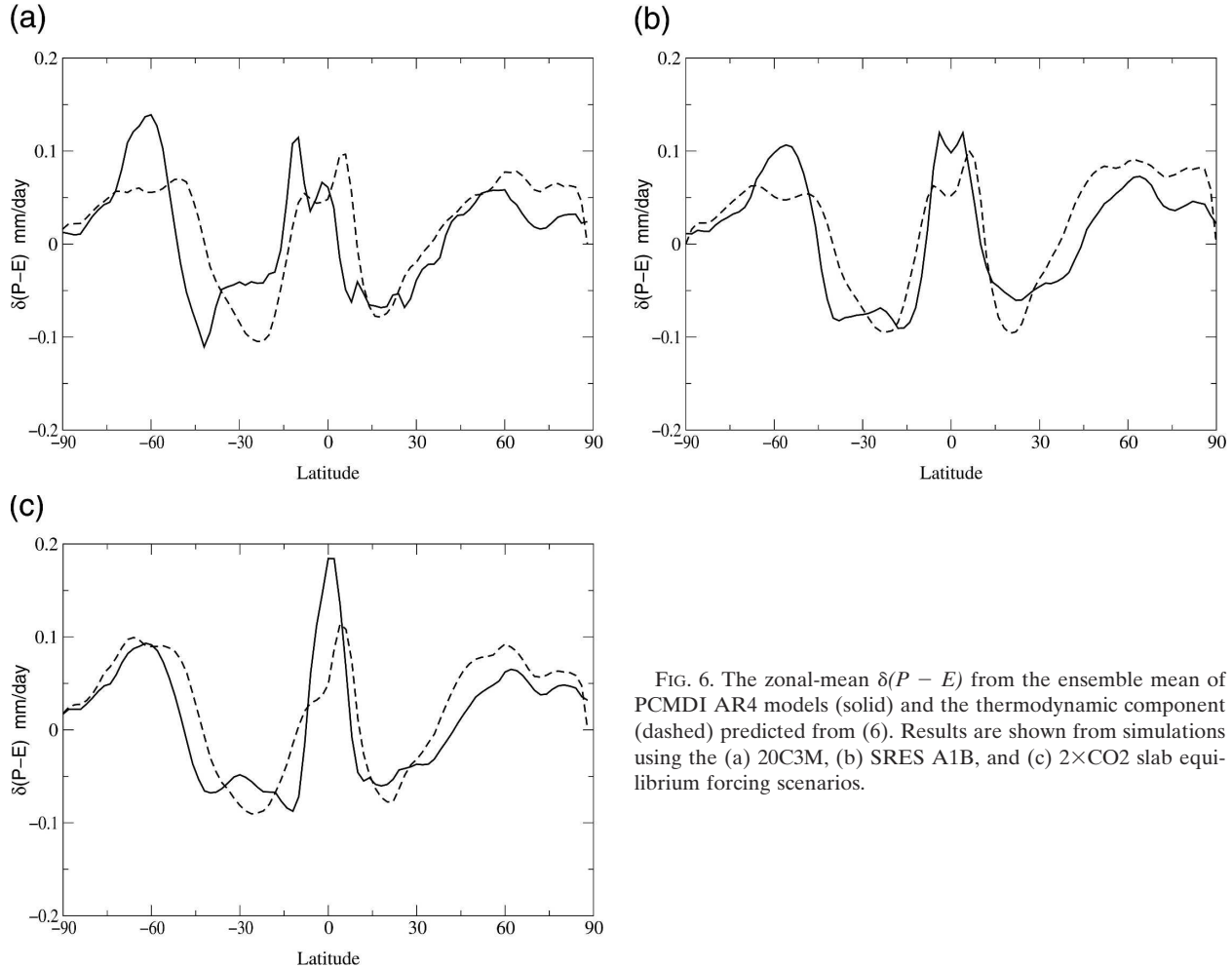
(a)

(b)

(c)

FIG. 6. The zonal-mean $\delta(P - E)$ from the ensemble mean of PCMDI AR4 models (solid) and the thermodynamic component (dashed) predicted from (6). Results are shown from simulations using the (a) 20C3M, (b) SRES A1B, and (c) 2×CO2 slab equilibrium forcing scenarios.

using the local rather than global-mean temperature responses, but it is apparent that the CC increase in vapor determines the basic structure of the response.

An increasing poleward moisture flux with increasing temperature is explicitly assumed or is implicitly generated in most simple energy balance climate models in which one tries to include the poleward moisture flux (e.g., Nakamura et al. 1994) and has been remarked upon in GCM global warming simulations since the inception of this field (Manabe and Wetherald 1975). It is reassuring but not surprising to find this behavior in the comprehensive AR4 models as well.

The result for precipitation minus evaporation is

$$\delta(P - E) = -\boldsymbol{\nabla} \cdot (\alpha \delta TF). \qquad (5)$$

If one can remove δT from the derivative, assuming that $P - E$ has more meridional structure than δT, then $P - E$ itself satisfies CC scaling:

$$\delta(P - E) = \alpha \delta T(P - E). \qquad (6)$$

The pattern of $P - E$ is simply enhanced, becoming more positive where it is already positive and more negative where it is negative.

One expects this simple balance to be most relevant over the oceans, where low-level relative humidity is strongly constrained, as well as over well-watered land regions. Over arid or semiarid land surfaces, changes in mean low-level relative humidity are not constrained to be small. In these regions, it is, rather, the runoff, $P - E$, and the flux divergence that are constrained to remain small. The approximation in (5) can potentially predict the unphysical result that $P - E < 0$ over land; the modified version (6) has the accidental advantage in this regard that it predicts that $P - E$ will simply remain small where it is already small.

Figure 6 shows the composited change in the zonal- and annual-mean $P - E$ and the change predicted by (6). We use the zonal- and annual-mean change in the surface air temperature, and simply assume that $\alpha = 0.07$ K^{-1} to predict a $\delta(P - E)$ distribution for each

model from its zonal- and annual-mean $P - E$, from (6). We then divide by the global-mean temperature change before averaging over all models to compute both the model and the predicted change in $P - E$ per unit global warming. There are three panels in the figure, corresponding to the change simulated by the AR4 models in the twentieth century (between the periods 1900–20 and 1980–2000; Fig. 6a), the change between the years 2000–20 and 2080–2100 in the A1B scenario (Fig. 6b), and the equilibrium response to a doubling of CO_2 in slab ocean versions of these models (Fig. 6c). The latter equilibrium responses with fixed (implied) oceanic heat fluxes are particularly distinguished from the transient integrations by much larger warming in high southern latitudes.

The fit, which has no free parameters, is rather impressive for these composites; it can be somewhat less accurate for individual models, presumably because the part of the response of $P - E$, related to changes in circulation and, potentially, relative humidity, differs from model to model more than does this simple thermodynamic component.

The fit is somewhat better than one might expect in fact, given the many simplifications made in the derivation, including the neglect of the correlation between F and δT in the seasonal cycle.

The difference between the actual response and this simple fixed flow–fixed relative humidity response clearly shows the effects of the poleward movement of the storm tracks in both hemispheres, which displaces the poleward boundary of the dry subtropical zones with $P - E < 0$ farther poleward. The differences between response and prediction are especially large over the Southern Ocean, where the increase in poleward moisture flux is underestimated, most substantially in the twentieth century. This overestimate in the Southern Hemisphere is reduced in the A1B twenty-first-century simulations, while in the equilibrated slab ocean runs, which allow the Southern Ocean to warm, the prediction is equally good in both hemispheres.

Given the discussion in the preceding section of the reduction in mass exchange between the boundary layer and the interior of the troposphere, especially in the Tropics, one might wonder why this prediction for the change in $P - E$, assuming no change in flow or low-level relative humidity, works as well as it does in the Tropics. If the mass flux in the Hadley cell were reduced in strength following CC scaling, for example, it should cancel the effects of increasing vapor and result in no increase in equatorial rainfall. Clearly this does not occur (although there is a tendency for the simple theory to overestimate the subtropical drying). We have argued that slowdown of the mean meridional

circulation need not follow the CC scaling of the reduction in the mass exchange, but we admit to being surprised that this simple expression works as well as it does in the zonal mean. A methodology for a more satisfying analysis of tropical precipitation responses to global warming is outlined by Chou and Neelin (2004). The fixed flow–fixed relative humidity response is but one term in their analysis.

Figure 7 shows the geographical distribution of the annual-mean change in $P - E$ as well as the prediction, $0.07 \delta T (P - E)$. Here δT is the local annual-mean temperature change. Once again, we composite across the models after normalization by the global-mean temperature response. While it is not accurate enough in isolation to be used as a basis for projections of regional hydrology, this simple thermodynamic constraint is clearly an important component of many regional changes, at least for subtropical to subpolar latitudes. The impression from this figure is that this thermodynamic constraint combined with a simple theory for the poleward expansion of the subtropics might provide a useful first approximation outside of the deep Tropics.

There are other interesting ways of dividing the local hydrologic response into "thermodynamic" and "dynamic" components—see, for example, Emori and Brown (2005), who also find a "dynamical" weakening of precipitation consistent with a reduction in convective mass flux.

To convert this prediction for $\delta(P - E)$ into a theory for δP, we need an expression for δE. A simple choice is to assume that the evaporation increases proportionally to the control evaporation. The global-mean increase in evaporation is 2% K^{-1} so the resulting expression for the precipitation response per unit global warming is

$$\delta P = 0.07 \, \delta T (P - E) + 0.02E. \qquad (7)$$

Figure 8 shows the result for the zonal means in the A1B runs for both δP and δE.

Because the interesting reduction in evaporation in the Southern Ocean is not captured by this simple fit to δE, the resulting fit for $\delta(P - E)$ substantially overestimates the increase in precipitation in these southern latitudes.

Droughts and floods can be thought of as produced by low-frequency variability in the flow field and therefore in the moisture transport. If we make the conservative assumption once again that the statistics of this variability remain unchanged while the magnitude of F increases, then the intensity of both floods and droughts will increase, as more water is transported by any particular anomalous flow from the region of anomalous vapor convergence to the region of anoma-
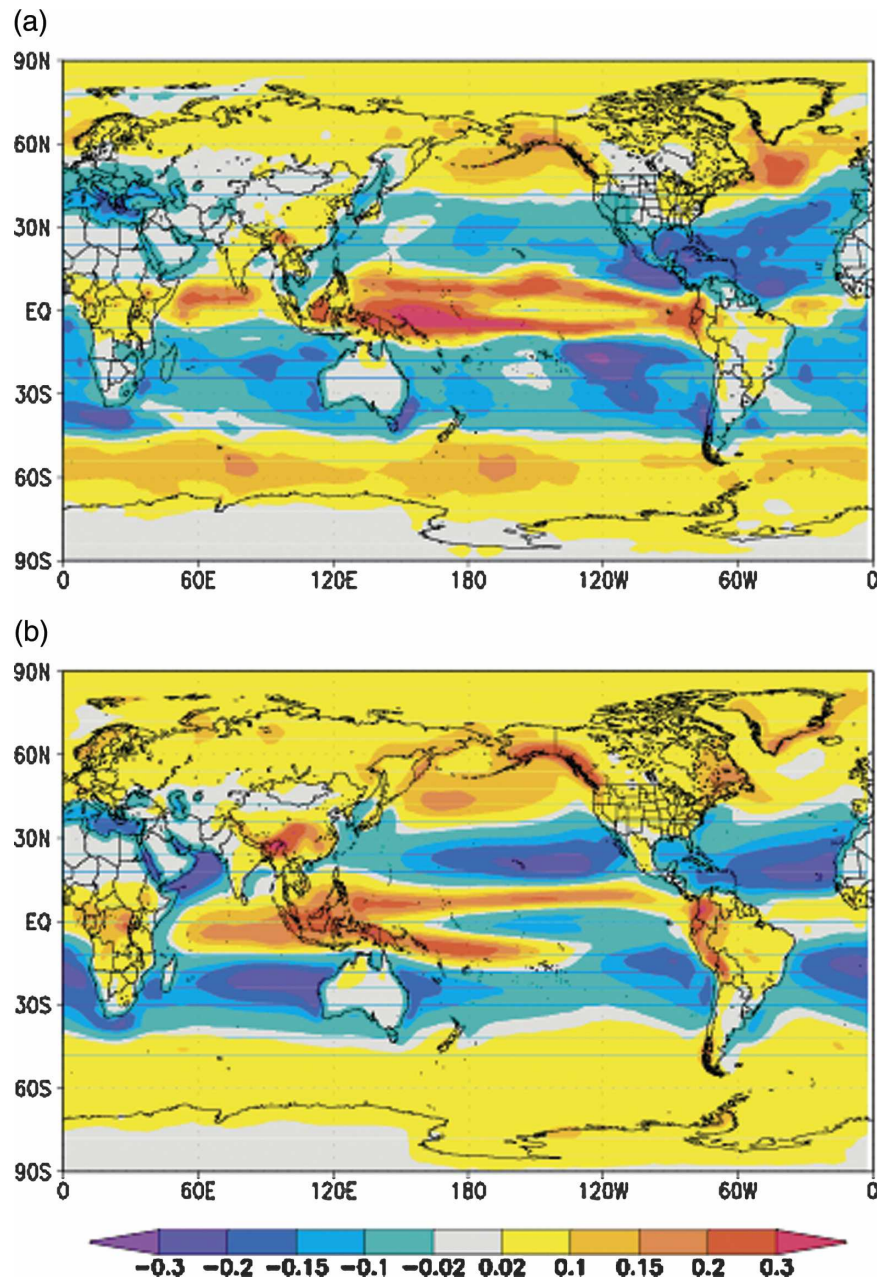
FIG. 7. The annual-mean distribution of $\delta(P - E)$ from the ensemble mean of (a) PCMDI AR4 models and (b) the thermodynamic component predicted from (6) from the SRES A1B scenario.

lous vapor divergence. Dry and marginal land areas, where sensitivity to drought is the greatest, are once again not strongly constrained by his kind of argument. Figure 9 shows the zonal-mean change in variance V of monthly mean anomalies in $P - E$ (local anomalies from the respective climatological seasonal cycles, with the zonal averaging performed after computing the local variance) and the CC scaling prediction: $\delta V/V \approx 2\alpha\delta T$. [See Raisanen (2005) for a related analysis of the

CMIP2 models.] The models' increase in variability is uniformly smaller than anticipated from CC scaling of the flux, a result that we are tempted to attribute to the weakening in the mass exchange discussed in section 4.

6. Poleward energy transport

The increased amplitude of the poleward vapor transport implies increased amplitude in the meridional
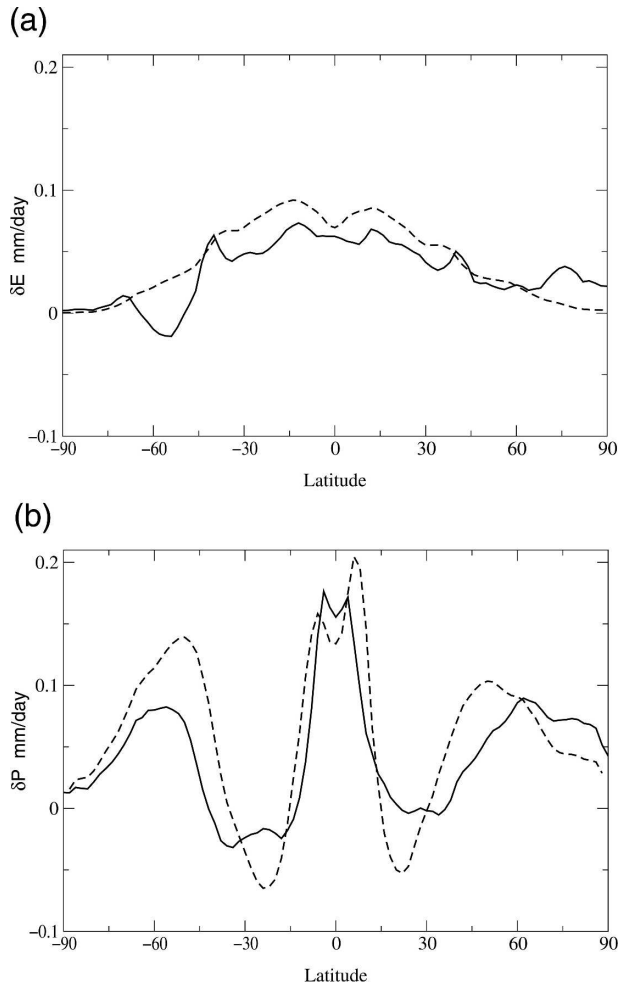
(a)

(b)

FIG. 8. The zonal-mean (a) δE and (b) δP from the ensemble mean of PCMDI AR4 models (solid) and the thermodynamic component (dashed) predicted from (7) from the SRES A1B scenario.

transport of latent energy. The total poleward energy transport is the sum of this latent energy transport plus the transport of dry static energy. It is of interest to examine the extent to which changes in sensible heat transport compensate for the changes in latent transport. This compensation is clearly seen in a variety of equilibrium responses of GCMs to warming and cooling [see the first such calculation in Manabe and Wetherald (1975)].

We first examine this compensation in the equilibrium responses to doubling CO_2 using the flux-adjusted slab ocean models. This is a simpler case than the transient warming experiments in that there is no change in the flux into the oceans. The composite over all models (Fig. 10a) shows the expected compensation. Since the latent transport is equatorward in the Tropics but poleward in midlatitudes, one sees an increased poleward dry static energy transport in the Tropics but a de-
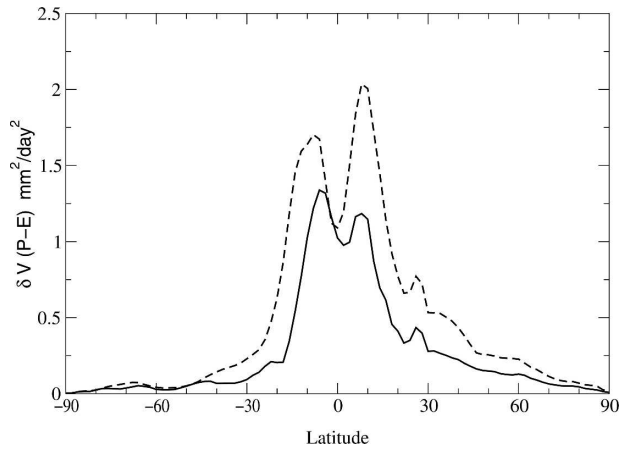

FIG. 9. The zonal-mean change in variance of monthly mean $(P - E)$, δV, from the ensemble mean of PCMDI AR4 models (solid) and the thermodynamic component (dashed) from the SRES A1B scenario.

creased transport in midlatitudes, a fundamental distinction between the tropical and extratropical responses to warming. The tropical increase is accomplished by an increase in the depth of the Hadley circulation and a reduction in the lapse rate, both of which contribute to the needed increase in the dry static energy difference between poleward and equatorward flows, overcompensating for any reduction in Hadley cell strength. The reduction in the extratropical poleward dry static energy transport is generated by a reduction in the eddy sensible heat transport.

If one inspects the magnitude of the total transport and its moist and dry components, one finds that the decrease in the sensible component compensates for about 70% of the latent transport increase at 45° latitude, near the maximum in the total transport. It would be of interest to try to understand this number, but here we are primarily concerned with the implications of this compensation for the CC scaling of the moisture transport. Returning to (4), rather than assuming that the eddy sensible heat transport is unchanged, we consider the implications of a compensation of given strength μ:

$$\delta F_S / F_S = \mu \delta F_L / F_L, \tag{8}$$

where $\mu \cong 0.7$ for these slab ocean simulations. We also need the ratio of latent to sensible transport in the unperturbed climate $F_L \equiv \xi F_S$. The constant ξ is a strong function of temperature and therefore of latitude. Its value is ≈ 1 at the maximum in the total transport. The resulting modification to CC scaling is

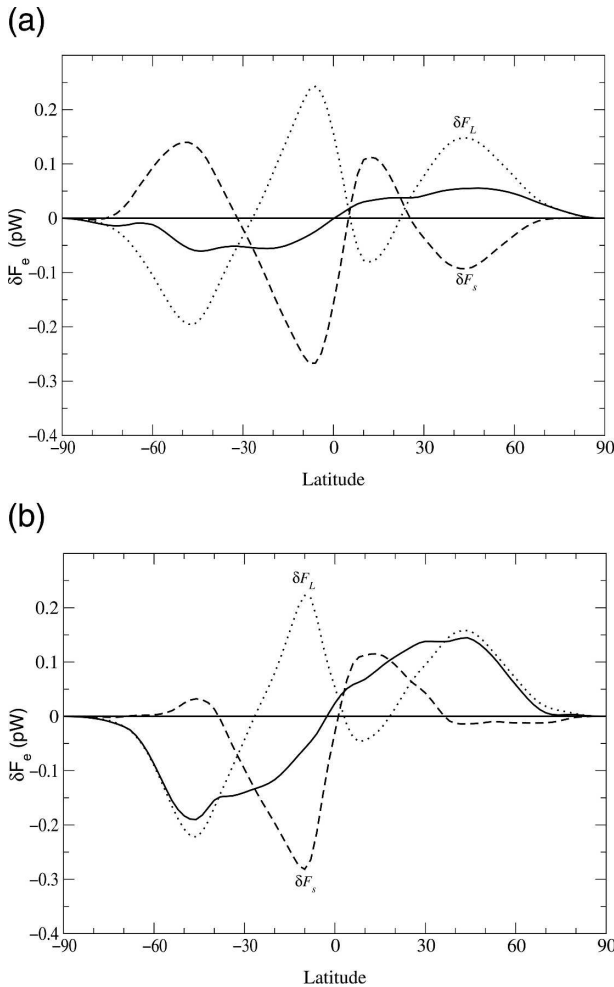$$\frac{\delta F_L}{F_L} \approx \frac{\alpha \delta T}{1 + \mu \xi}. \tag{9}$$

(a)

(a)

(b)

(b)

FIG. 10. The change in zonal-mean northward atmospheric energy transports (a) from 2×CO2 slab equilibrium simulations and (b) from SRES A1B transient simulations. Results are shown for the total atmospheric energy transport (solid), the sensible energy transport δF_s (dashed), and the latent energy transport δF_L (dotted).

FIG. 11. The change in zonal-mean energy transports for the atmosphere δF_a (dashed), ocean δF_o (dotted), and atmosphere + ocean (solid) from (a) the 2×CO2 slab equilibrium simulations and (b) SRES A1B simulations. The oceanic contribution includes the differential heat storage, as described in the text.

The expression predicts that the increase in the extratropical moisture flux will be about 60% of the CC scaling value at 45° latitude. This estimate is only meant as a rough indication of how much difference we might expect between models in which the increased latent flux is compensated by a decrease in the sensible flux and models in which there is no compensation. As one moves poleward, ξ decreases, and the effects of compensation on the latent flux response should be smaller.

Turning to the integrations for the A1B transient scenario, the results for the heat fluxes are provided in Fig. 10b. A surprising result here is that there is little or no compensation of the increased extratropical latent flux in either hemisphere. The difference between the transient warming scenario and the equilibrated slab ocean
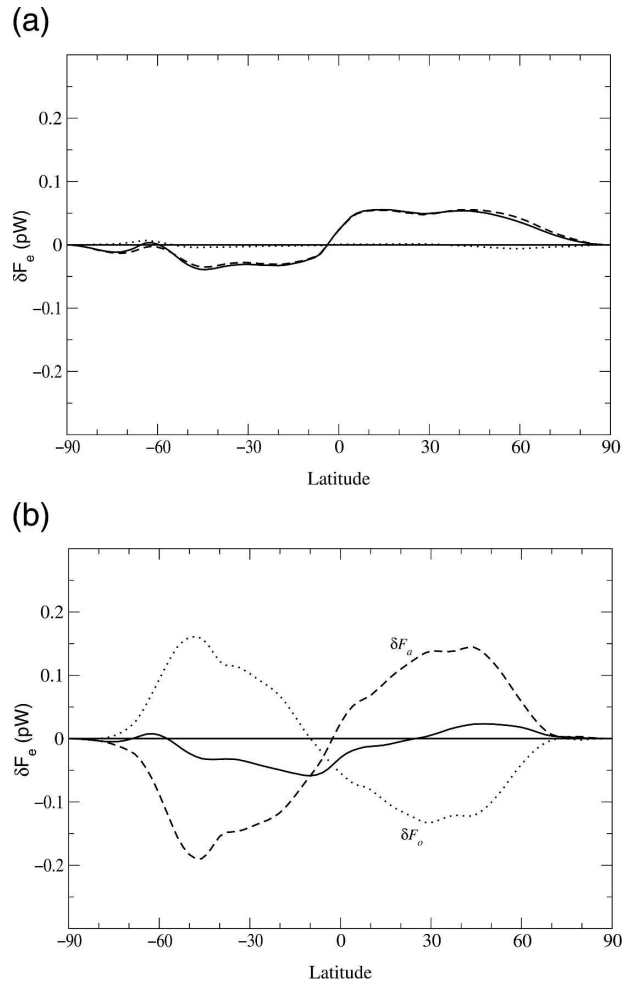
models in this respect is striking. Inspection of the fluxes at the top of the atmosphere (Fig. 11) shows that this increased total atmospheric poleward flux in the transient experiments is not radiating out the top of the atmosphere but is passed to the oceans instead. In constructing this figure, we first take the flux into the ocean, remove its global mean, and then integrate from one pole to the other, yielding the sum of ocean transport and differential heat storage. The change in this quantity is the dotted line labeled "ocean" in the figure. The "total" is the sum of this ocean contribution and the change in atmospheric transport and can be computed by integrating the fluxes at the top of the atmosphere, after removing the global mean. One sees that the changes in the top of atmosphere fluxes are not very different than in the slab ocean case. It is the oceanic

contribution that compensates the increased latent transport in the extratropics in the transient warming, rather than a reduction in sensible transport. This oceanic differential storage plus transport should, therefore, obey CC scaling.

One lesson that this result provides is that it is not that the atmosphere prefers to maintain the same total atmospheric flux, but that it prefers not to change the basic gradient in the top-of-the-atmosphere net radiative flux. In the face of the unavoidable increase in the poleward extratropical latent heat transport, in the equilibrated system there is no alternative but a decrease in the sensible transport. In the transient case, one can divide the necessary adjustment between the sensible heat transport and differential oceanic heat storage plus transport. If we assume that the sensible heat transport reacts to changes in meridional temperature gradients, it is plausible that the reduction of the sensible heat transport in the Southern Hemisphere in the transient experiments is retarded, since the Southern Ocean temperatures are very slow to warm and the resulting increased meridional gradient would work against any such reduction. What is unanticipated is that the results look very similar in the Northern and Southern Hemispheres, despite the polar amplification at low levels and the resulting reduction in the meridional gradient in the Northern Hemisphere. One possible interpretation is that the polar amplification over land has little impact on the oceanic storm tracks where much of the heat transport takes place.

On the basis of the diffusive picture leading to (9), one would expect a model with compensation to show a smaller response in the moisture flux, per unit warming, than a model without compensation. This does seem to be the case in the Southern Hemisphere in Fig. 6, since the scaled $P - E$ decreases as one moves from the twentieth century and A1B simulations to the equilibrium slab runs, but the results in the Northern Hemisphere are less clear. These distinctions between equilibrated and transient simulations are deserving of closer examination.

7. Conclusions

A number of important aspects of the hydrological response to warming are a direct consequence of the increase in lower-tropospheric water vapor. Because the increase in strength of the global hydrological cycle is constrained by the relatively small changes in radiative fluxes, it cannot keep up with the rapid increase in lower tropospheric vapor. The implication is that the exchange of mass between boundary layer and the midtroposphere must decrease, and, since much of this

exchange occurs in moist convection in the Tropics, the convective mass flux must decrease. In many popular, and in some scientific, discussions of global warming, it is implicitly assumed that the atmosphere will, in some sense, become more energetic as it warms. By the fundamental measure provided by the average vertical exchange of mass between the boundary layer and the free troposphere, the atmospheric circulation must, in fact, slow down. This large-scale constraint has little direct relevance to the question of how tropical storms will be affected by global warming, since the mass exchange in these storms is a small fraction of the total tropical exchange.

In contrast, assuming that the lower-tropospheric relative humidity is unchanged and that the flow is unchanged, the poleward vapor transport and the pattern of evaporation minus precipitation $(E - P)$ increases proportionally to the lower-tropospheric vapor, and in this sense wet regions get wetter and dry regions drier. Since the changes in precipitation have considerably more structure than the changes in evaporation, this simple picture helps us understand the zonally averaged pattern of precipitation change. In the extratropics, one can alternatively think of the diffusivity for vapor and for sensible heat as being the same, with similar consequences for the change in the vapor transport. If one assumes that the statistics of the flow are also unchanged, one obtains estimates of the increase in variance of $E - P$ (the increased intensity of "droughts and floods") that are reasonable but overestimate the response of the model variances, perhaps because of the decrease in the strength of the mass exchange.

In the Tropics, one confidently expects compensation between the increase in the equatorward latent heat transport and an increase in poleward dry static energy transport; otherwise the net transport in the Tropics would change sign. One also expects a decrease in the poleward sensible heat flux in the extratropics, as seen in many previous GCM studies. Surprisingly we see this decrease only in the equilibrium climate response as estimated with slab ocean models, and not in the transient climate change experiments. Particularly intriguing is the response in the Northern Hemisphere, where there is no reduction in the sensible heat transport despite the reduction in the zonal-mean temperature gradient at low levels associated with polar amplification of the warming. An implication of this result is that one can estimate the differential oceanic heat storage plus transport (the heat entering the ocean, with the global mean removed) directly from the Clausius–Clapeyron-dominated response of the latent heat transport.

To the extent that we have simple plausible physical

arguments that support the model consensus, we believe that one should have nearly as much confidence in these results as one has in the increase in temperature itself.

REFERENCES

Allen, M. R., and W. J. Ingram, 2002: Constraints on future changes in the hydrological cycle. *Nature,* **419,** 224–228.

Betts, A. K., 1998: Climate–convection feedbacks: Some further issues. *Climatic Change,* **39,** 35–38.

Boer, G. J., 1993: Climate change and the regulation of the surface moisture and energy budgets. *Climate Dyn.,* **8,** 225–239.

Bosilovich, M. G., S. D. Schubert, and G. K. Walker, 2005: Global changes in water cycle intensity. *J. Climate,* **18,** 1591–1608.

Chou, C., and J. D. Neelin, 2004: Mechanisms of global warming impacts on regional tropical precipitation. *J. Climate,* **17,** 2688–2701.

Emori, S., and S. J. Brown, 2005: Dynamic and thermodynamic changes in mean and extreme precipitation under changed climate. *Geophys. Res. Lett.,* **32,** L17706, doi:10.1029/ 2005GL023272.

GFDL Global Atmospheric Model Development Team, 2004: The new GFDL global atmosphere and land model AM2– LM2: Evaluation with prescribed SST simulations. *J. Climate,* **17,** 4641–4673.

Held, I. M., and B. J. Soden, 2000: Water vapor feedback and global warming. *Annu. Rev. Energy Environ.,* **25,** 441–475.

Knutson, T. R., and S. Manabe, 1995: Time-mean response over the tropical Pacific to increase CO_2 in a coupled ocean– atmosphere model. *J. Climate,* **8,** 2181–2199.

Lindzen, R. S., A. Y. Hou, and B. F. Farrell, 1982: The role of convective model choice in calculating the climate impact of doubling CO_2. *J. Atmos. Sci.,* **39,** 1189–1205.

Manabe, S., and R. T. Wetherald, 1975: The effect of doubling CO_2 concentration on the climate of the general circulation model. *J. Atmos. Sci.,* **32,** 3–15.

Mitas, C. M., and A. Clement, 2005: Has the Hadley cell been strengthening in recent decades? *Geophys. Res. Lett.,* **32,** L03809, doi:10.1029/2004GL021765.

Nakamura, M., P. H. Stone, and J. Marotzke, 1994: Destabilization of the thermohaline circulation by atmospheric eddy transports. *J. Climate,* **7,** 1870–1882.

Pierrehumbert, R. T., 2002: The hydrologic cycle in deep time climate problems. *Nature,* **419,** 191–198.

Raisanen, J., 2005: Impact of increasing CO_2 on monthly-to-annual precipitation extremes: Analysis of CMIP2 experiments. *Climate Dyn.,* **24,** 309–323.

Ramanathan, V., P. J. Crutzen, J. T. Kiehl, and D. Rosenfeld, 2001: Aerosols, climate and the hydrological cycle. *Science,* **294,** 2119–2124.

Roads, J. O., S. C. Chen, S. Marshall, and R. Oglesby, 1998: Atmospheric moisture cycling rates. *GEWEX News,* Vol. 8, Internatinal GEWEX Project Office, 7–10.

Santer, B. D., and Coauthors, 2005: Amplification of surface temperature trends and variability in the tropical atmosphere. *Science,* **309,** 1551–1556.

Soden, B. J., and I. M. Held, 2006: An assessment of climate feedbacks in coupled atmosphere–ocean models. *J. Climate,* **19,** 3354–3360.

Trenberth, K. E., 1998: Atmospheric moisture residence times and cycling: Implications for rainfall rates with climate change. *Climatic Change,* **39,** 667–694.

——, J. Fasullo, and L. Smith, 2005: Trends and variability in column integrated atmospheric water vapor. *Climate Dyn.,* **24** (7–8), 741–758.

Wentz, F. J., 1997: A well-calibrated ocean algorithm for SSM/I. *J. Geophys. Res.,* **102,** 8703–8718.

——, and E. A. Francis, 1992: Nimbus-7 SMMR Ocean Products, 1979–1984. Remote Sensing Systems Tech. Rep. 033192, Santa Rosa, CA, 36 pp.

——, and M. Schabel, 2000: Precise climate monitoring using complementary data sets. *Nature,* **403,** 414–416.

Winton, M., 2006: Surface albedo feedback estimates for the AR4 climate models. *J. Climate,* **19,** 359–365.